



Grafted multifunctional titanium dioxide nanotube membrane: Separation and photodegradation of aquatic pollutant

Xiwang Zhang ^{a,*}, Alan Jianhong Du ^a, Peifung Lee ^a, Darren Delai Sun ^{a, **}, James O. Leckie ^b

^a School of Civil and Environmental Engineering, Nanyang Technological University, Singapore 639798, Singapore

^b Department of Civil and Environmental Engineering, School of Engineering, Stanford University, Stanford, CA 94305-4020, USA

ARTICLE INFO

Article history:

Received 14 December 2007

Received in revised form 23 March 2008

Accepted 6 April 2008

Available online 18 April 2008

Keywords:

Nanotube

Titanium dioxide

Membrane

Photodegradation

Fouling

ABSTRACT

Titanium dioxide (TiO_2) nanotube membrane has been fabricated by an energy efficient and environmentally friendly method, grafting anatase TiO_2 nanotubes in the channels of alumina microfiltration (MF) membrane using TiF_4 solution through liquid-phase deposition. The inner diameters of the TiO_2 nanotubes are controllable from 5 to 100 nm by varying the grafting time. The TiO_2 nanotube membrane exhibited good photocatalytic activity on photodegradation of HA (humic acid) in batch tests. The satisfying permeability of the TiO_2 nanotube membrane was demonstrated by filtration of distilled water and HA. The experiment results of continuous filtration under UV irradiation showed that not only HA was rejected and photodegraded by the TiO_2 nanotube membrane, but also the membrane fouling was alleviated dramatically.

© 2008 Elsevier B.V. All rights reserved.

1. Introduction

New and increasingly stringent regulations for the discharge of effluents require a more reliable and sustainable treatment process. The membranes separation of gases and liquids can often be more economical and energy effective than traditional separation methods, such as distillation or absorption [1]. Smaller size, easier maintenance and superior separation efficiency ensure membrane as a promising alternative to conventional water and wastewater treatment processes as well as air-purification and gas-separation processes. An ideal membrane would have excellent stability under a wide range of process conditions, high selectivity for the chemicals of interest, and also produce a large molecular flux with a small driving force. Most of the membranes currently used in industries are polymeric, and fabrication of these devices is highly developed. However, polymeric membranes are unsuitable for high temperature, acid or alkali applications. Inorganic membranes have attracted considerable attention due to their excellent thermal, chemical, mechanical stability, and their reusability after burning over conventional polymeric membranes [2]. In particular, its stable pore size ensures the consistency of the

permeate quality. Among the materials used for the preparation of inorganic membranes, TiO_2 have gained tremendous popularity due to its excellent properties under UV irradiation; ability to mineralize virtually all organic compounds and to inactivate pathogenic microorganisms present in contaminated water [3–7]. This means that unlike other ceramic membranes, TiO_2 membrane has multifunctional characters such as separation, photocatalytic degradation of organic foulants on membrane surface and disinfection [8]. Since the pioneering work on the TiO_2 photocatalytic membrane by Anderson and co-workers using sol-gel method [9,10], many research studies have been carried out to fabricate TiO_2 membranes by coating TiO_2 films on various supports [2,11–24]. However, these TiO_2 membranes usually need high driving force due to their interlaced channels in TiO_2 layer.

Since the discovery of carbon nanotubes [25], synthesis and characterization of one-dimensional nanostructures, in particular nanotubular symmetries, have attracted significant scientific and technological interests in the last decade. The possibility of using nanotubes as membranes for separation has been recognized for some time. The first examinations of this idea used molecular dynamics simulations of gas transport inside single-walled nanotubes [26,27]. These simulations predicted that the transport of gases inside nanotubes is in orders of magnitude faster than in any other known materials with nanometer-scale pores. Holt et al. have fabricated the first membrane from aligned single- and double-walled nanotubes [28]. This work follows similar experiments by Hinds and co-workers with membranes made from multiwalled nanotubes [29,30]. These experiments ascertain that

* Corresponding author at: School of Civil and Environmental Engineering, Nanyang Technological University, Blk N1, N1-B4b-03, 50 Nanyang Avenue, Singapore 639798, Singapore. Tel.: +65 6790 6914; fax: +65 6861 5254.

** Corresponding author. Tel.: +65 6790 6273; fax: +65 6791 0676.

E-mail addresses: xwzhang@ntu.edu.sg (X.W. Zhang), ddsun@ntu.edu.sg (D.D. Sun).

membrane of nanotube arrays can have unusually high fluxes. Moreover, several studies have indicated that titania in the form of nanotube has improved photocatalytic properties compared to any other forms of titania for application in photocatalysis [31,32]. Hence, TiO_2 nanotube membrane has great potential in environmental purification.

Titania nanotubes have been produced by a variety of methods including sol-gel transcription using organo-gelators as templates [33,34], seeded growth [35], anodization [36–38] and hydrothermal processes [39–41]. However, the above-mentioned methods are difficult to mass produce in a cost-efficient manner. Direct grafting TiO_2 film using supersaturated titanium tetrafluoride (TiF_4) solution has been developed on various substrates [42,43]. Imai et al. found the method in producing TiO_2 nanotube to be efficient and facile [44,45]. In the present work, we describe the preparation of a TiO_2 nanotube membrane by direct grafting TiO_2 nanotube in the channels of alumina membrane using supersaturated TiF_4 solution. Its potential application was discussed by investigating its photocatalytic activity and permeability.

2. Experimental

2.1. Synthesis of TiO_2 nanotube membrane

TiF_4 (Aldrich) was dissolved in deionized water under strong magnetic stirring to gain a 0.04 M solution. After the pH of the 0.04 M TiF_4 solution was adjusted to 2.2 using ammonia solution (1 M), alumina membranes (Whatman, pore size: 200 nm) was immersed into the above TiF_4 solution for a desired period of time to graft TiO_2 on alumina membranes. Then the alumina membranes were dried at room temperature. Before used, alumina membranes were washed H_2SO_4 (0.1 M) and deionized water, respectively. The as-prepared TiO_2 nanotube membrane was gained after the grafted TiO_2 film on alumina membrane surface was removed using sand paper.

2.2. TiO_2 nanotube membrane characterization

The morphologies of the membranes were quantified using images from the field-emission scanning electron microscope (FESEM) Jeol (Japan) JSM-6340F at an accelerating voltage of 5 kV. Pt coating (20 mA, 30 s) was applied to the membranes during the imaging. Secondary electrons mode was employed unless otherwise stated. X-ray diffraction (XRD) patterns were obtained using Bruker (Germany) AXS D8 Advance ($\text{Cu K}\alpha$ $\lambda = 1.5406 \text{ \AA}$). The scanning rate was $0.03^\circ \text{ s}^{-1}$ in 2θ mode from 20° to 70° . XRD analysis of TiO_2 nanotube is not possible due to the configuration of the membrane. Titania nanotubes are within the channels of the alumina membrane. Alternatively, TiO_2 was grafted onto a glass slide under otherwise same conditions. The TiO_2 powder removed from the glass slide was used for XRD analysis in place of the TiO_2 nanotube membrane. The crystallinity of the TiO_2 should not be affected by this method.

2.3. Evaluation of photocatalytic activity and permeability of TiO_2 nanotube membrane

The photocatalytic activity and anti-fouling ability of the TiO_2 nanotube membrane was investigated in the homemade filtration setup as shown in Fig. 1. A glass filter cup (250 mL) was used as reactor. TiO_2 nanotube membrane was put on the bottom of the filtration cup. A pump connected the filter cup provided driving force for filtration. Membrane permeate was collected in a beaker and its volume was recorded by measuring its weight, which are controlled by a computer. The membrane flux can be calculated by

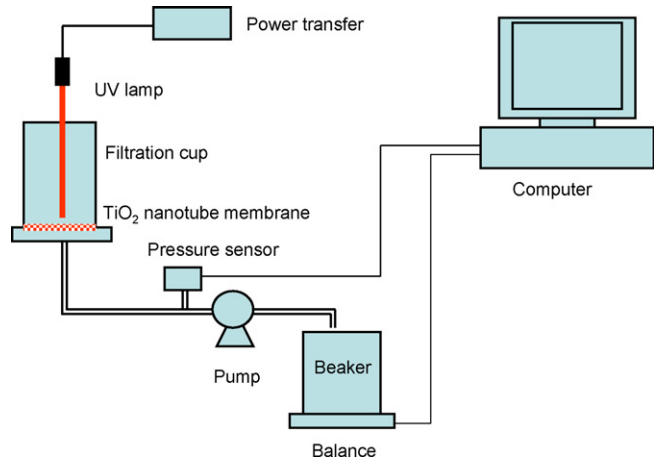


Fig. 1. Schematic diagram of evaluating photocatalytic activity and anti-fouling ability of the TiO_2 nanotube membrane.

the following equation:

$$J = \frac{\nabla V}{A \cdot \nabla t} \quad (1)$$

where J is permeation flux, ∇V the volume change of permeate, A the area of membrane, and ∇t is the filtration time.

Humic acid (HA, Fluka) was chosen as the model pollutant. HA solution was prepared in deionized water. The UV light source, an 11 W Upland 3SC9 Pen-ray lamp (254 nm) was immersed into solution, 1 cm above the TiO_2 nanotube membrane. First, the photocatalytic activity of the TiO_2 nanotube membrane was evaluated in batch operation mode. That is, during photocatalytic reaction the filtrate pump was off so that no solution passed through the membrane. HA solution of 15 mg/L was added in to the filter cup, and then turned on the UV lamp. Samples were withdrawn from the filter cup using a syringe at intervals of 15 min for analyses. HA concentration in samples was measured by monitoring the absorbance at 436 nm on a UV-vis spectrophotometer (Shimadzu UV-1700, Japan), and the total organic matter (TOC) concentration was measured on a Shimadzu TOC-Vcsh TOC analyzer. A commercial TiO_2 P25 (Degussa) deposited glass filter, which was prepared by depositing 0.05 g P25 on the surface of the glass filter ($0.45 \mu\text{m}$) via filtering P25 suspension, was used as a reference. The direct photolysis of HA under UV irradiation was also carried out. The permeability of the TiO_2 nanotube membrane was evaluated in a Millipore UF Stirred Cell. The anti-fouling ability of the TiO_2 nanotube membrane were investigated in the homemade filtration setup in continuous operation way. That is, during photocatalytic reaction the filtrate pump was on so that solution could pass through the membrane. There are concurrent photocatalytic degradation and separation in continuous operation way. HA solution of 15 mg/L was filtered under UV irradiation. The HA concentration and TOC both in feed and in filtrate were measured to calculate their removal rates.

3. Results and discussion

Fig. 2 shows FESEM image of the as-prepared TiO_2 nanotube membrane after 2 h of grafting. It was found that nanotubes were lined within the channels of alumina membrane. Chemical composition of the nanotubes was analyzed using EDX and the result is shown in Fig. 3. Titanium related compounds are detected in the nanotubes. The hypothesized anatase phase was confirmed with XRD (Fig. 4). The diffraction pattern reveals characteristic

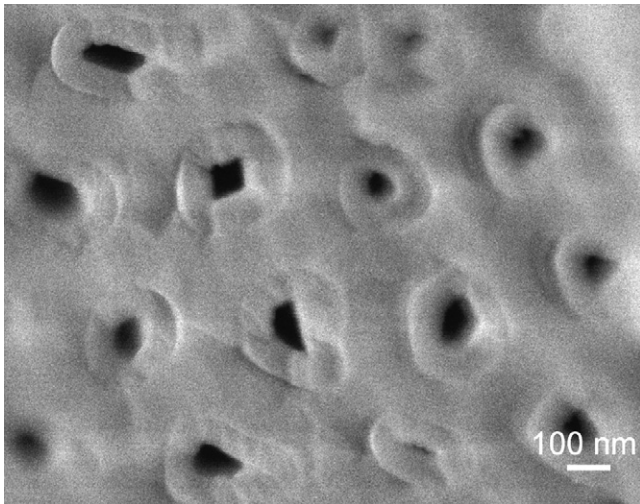


Fig. 2. FESEM image of the TiO_2 nanotube membrane after 2 h of grafting.

peaks of the anatase phase (JCPDS No. 21-1272). The results are consistent with previous studies [44,45]. As shown in Fig. 2, the walls of these TiO_2 nanotubes are about 40–60 nm in thickness and 50–70 nm in inner diameter. So, the membrane should be characteristically UF membranes. The average crystal size of the sample has been estimated by using Scherrer's formula, which is shown in the following equation:

$$D = \frac{0.89\lambda}{B(2\theta)\cos\theta} \quad (2)$$

In which $B(2\theta)$ is the width of the XRD peak at half-peak height in radians, λ the X-ray wavelength in nanometers and θ is the angle between the incident and diffracted beams in degrees. The crystal size is estimated to be around 5.4 nm.

A systematic study on varying the fabrication parameters has suggested that (a) the acid treatment of the as-received alumina membrane using 2% sulfuric acid promotes grafting of TiO_2 nanotube; (b) the pH of solution has strong effect on nanotube packing. Under the low-pH condition (pH less than 2), the deposition rate is slow but the TiO_2 coating is tightly packed. At high pH condition (pH more than 2.5), however, the deposition rate

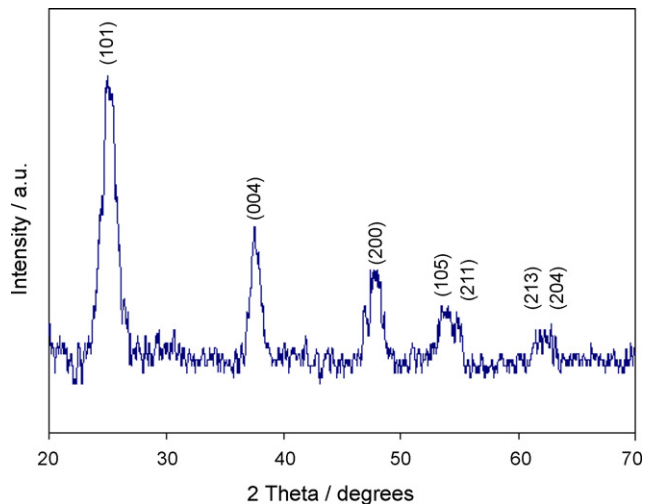


Fig. 4. XRD pattern of the TiO_2 deposited from TiF_4 solution.

is fast but the TiO_2 coating is loose; (c) inner diameter of TiO_2 nanotubes can be easily controlled by varying the deposition time. Long deposition time reduces the inner diameter of nanotubes by increasing the wall thickness of nanotubes. Fig. 5 shows FESEM image of the TiO_2 nanotube membrane after 4 h of grafting. It was found that the inner diameter of TiO_2 nanotubes decreased to 5–10 nm while the wall thickness of nanotubes increased about 30 nm to 80–90 nm due to extending deposition time. In the first 2 h, wall thickness of nanotube increased 40–60 nm while in second 2 h the thickness increased only 30 nm. That indicates that the grafting rate was not a constant. It decreased with grafting time.

Fig. 6 shows the mechanistic model of the formation of TiO_2 nanotubes from TiF_4 solution. The hydrolysis of TiF_4 in solution occurs in a stepwise manner to produce titania.



TiO_2 produced by the stepwise reaction in supersaturated TiF_4 solution at pH 1–3, thin crystalline films of TiO_2 are grafted through the heterogeneous nucleation on substrates [44,45]. The TiO_2 films in channels of alumina membrane would form nanotubes as shown in Fig. 6. With increasing grafting time, the

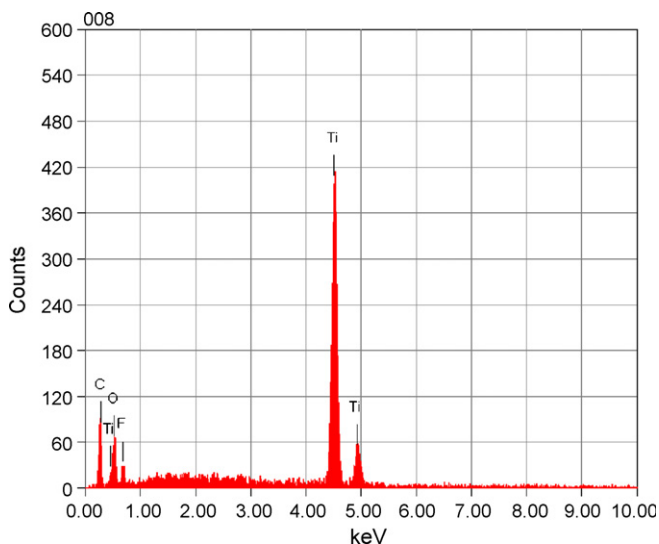


Fig. 3. Typical EDX microanalysis on TiO_2 nanotube.

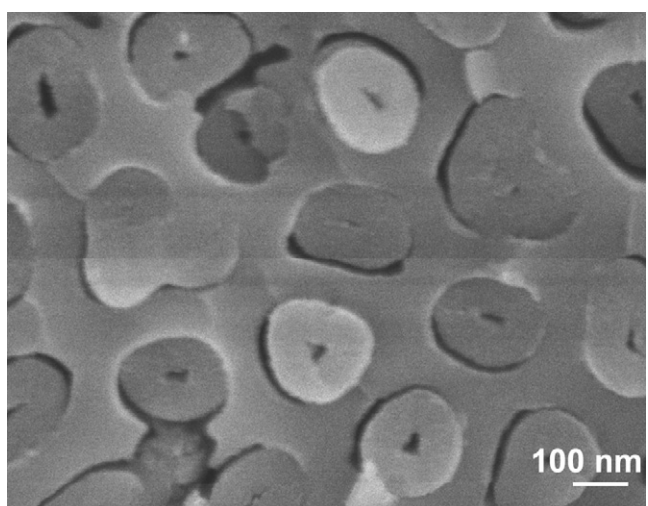


Fig. 5. FESEM image of the TiO_2 nanotube membrane after 4 h of grafting.

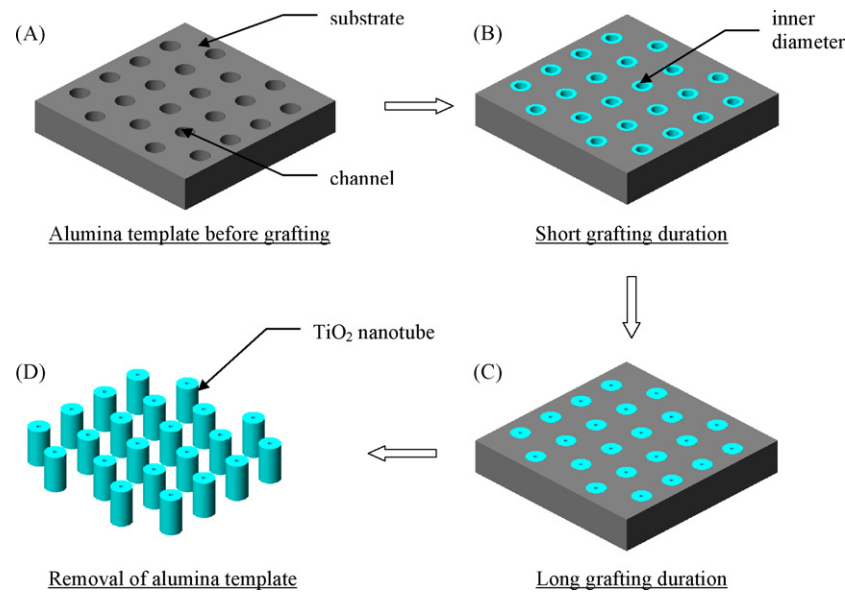


Fig. 6. Mechanistic model of the formation of TiO_2 nanotube membrane in channels of alumina membrane.

wall of TiO_2 nanotubes become thicker because more TiO_2 was grafted, hence, resulting in the reduction of inner diameter of these nanotubes.

The alumina membrane as template was subsequently removed by immersing the grafted membrane in the ammonia solution for several days at the room temperature. Fig. 7 shows FESEM image of TiO_2 nanotubes after alumina membrane was removed. The free-standing TiO_2 nanotube membrane becomes friable without the alumina substrate. Hence, it is more practical to utilize TiO_2 nanotubes together with alumina membrane as a support substrate.

The photocatalytic activity of the TiO_2 nanotube membrane was investigated in batch operation mode. The P25 deposited glass filter was used as a reference and the direct photolysis of HA under UV irradiation was also carried out as a blank. The changes in HA concentration and TOC over the course of the three processes are shown in Fig. 8. The TiO_2 nanotube membrane showed satisfying photocatalytic activity, which was slightly lower than that of commercial P25. The photocatalytic degradation of HA in the processes follow first-order kinetics. The apparent rate constant (k)

for the TiO_2 nanotube membrane and P25 are 0.017 and 0.023 min^{-1} , respectively. The TOC curves in Fig. 8 also show similar results. Compared with the photocatalytic degradation in the presence of either the TiO_2 nanowire or P25, the degradation of HA by photolysis without catalyst was much slow and the apparent rate constant was only 0.006 min^{-1} , being one-third of that of the photocatalytic degradations. This indicates that most of HA in TiO_2 nanotube membrane system were degraded by the photocatalysis rather than the photolysis.

To investigate the permeability of the TiO_2 nanotube membrane, membrane fluxes of distilled water under different TMP (transmembrane pressure) were investigated in Millipore UF Stirred Cell. The results were shown in Fig. 9, which indicates that the TiO_2 nanotube membrane has lower membrane flux than the alumina membrane without TiO_2 grafting due to its smaller pore size. Flux of TiO_2 nanotube membrane is proportional to the grafting time. As discussed above longer grafting time result in smaller pore size, hence lower flux. Although the membrane flux of the TiO_2 nanotube membrane is low, high separation efficiency is

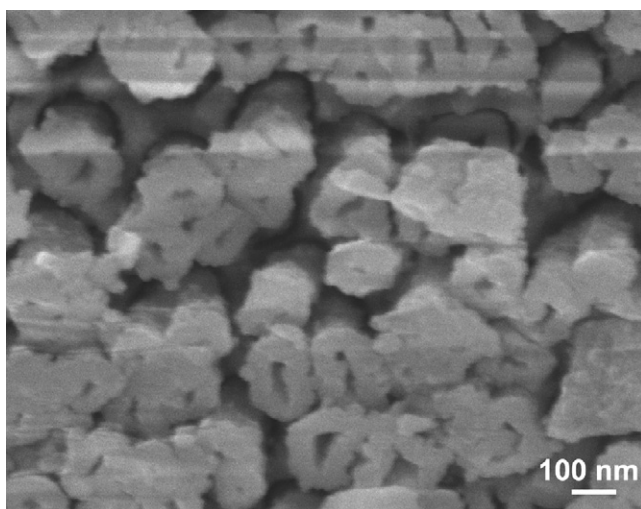


Fig. 7. FESEM image of TiO_2 nanotubes after removal of alumina substrate.

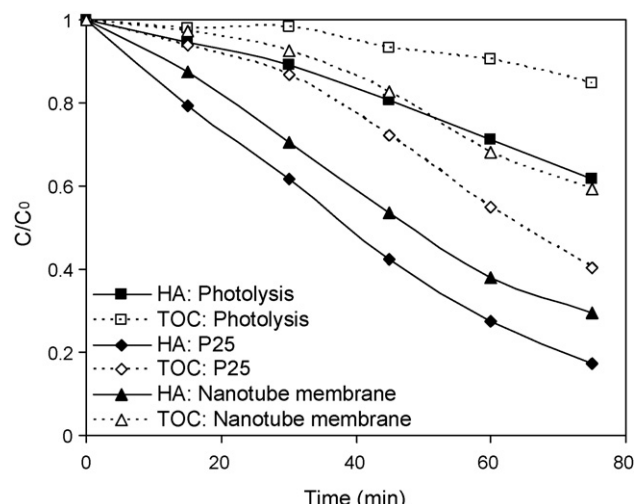


Fig. 8. Changes in HA concentration and TOC over the courses of photolysis, P25 deposited glass filter photocatalysis and TiO_2 nanotube membrane photocatalysis.

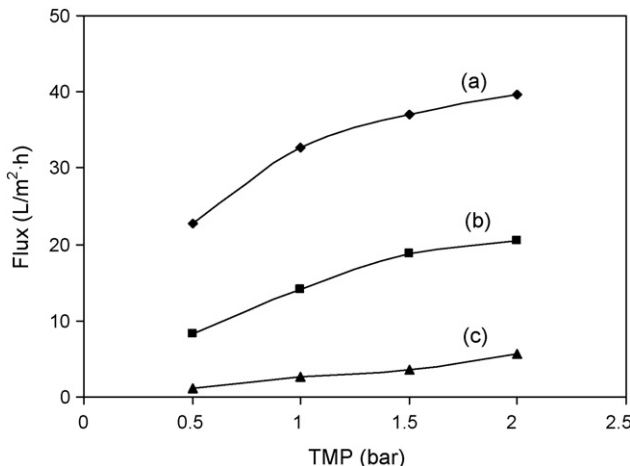


Fig. 9. Distilled water permeability of (a) alumina membrane, (b) TiO₂ nanotube membrane after 2 h of TiO₂ grafting and (c) TiO₂ nanotube membrane after 4 h of TiO₂ grafting.

achieved. HA solution was filtered by the TiO₂ nanotube membrane and removal rates of HA are shown in Fig. 10. The removal rate of HA using the TiO₂ nanotube membranes after 2 and 4 h grafting are 95.9% and 69.1%, respectively, much higher than that of alumina membrane (21.3%). Moreover, the TiO₂ nanotube membrane can degrade pollutants under UV irradiation rather than just rejecting the pollutants spatially like traditional membrane. Pollutants forming cake layer on membrane surface and blocking membrane pore are the major reasons of membrane fouling during filtration. Using this TiO₂ nanotube membrane for filtration, the membrane fouling would be alleviated dramatically because pollutants could be degraded. The anti-fouling ability of the TiO₂ nanotube membrane was investigated by measuring membrane fluxes during filtration of HA with and without UV irradiation. The TiO₂ nanotube membrane grafted for 2 h was used and the results were shown in Fig. 11. After 8 h of filtration, the membrane flux only decreased 27% with UV irradiation whereas the membrane flux decreased 67% without UV irradiation. The HA concentration and TOC in permeates were measured to evaluate their removal rates by the concurrent filtration and photocatalytic oxidation. Near 100% and 94.5% removal rates for HA and TOC, respectively, were achieved.

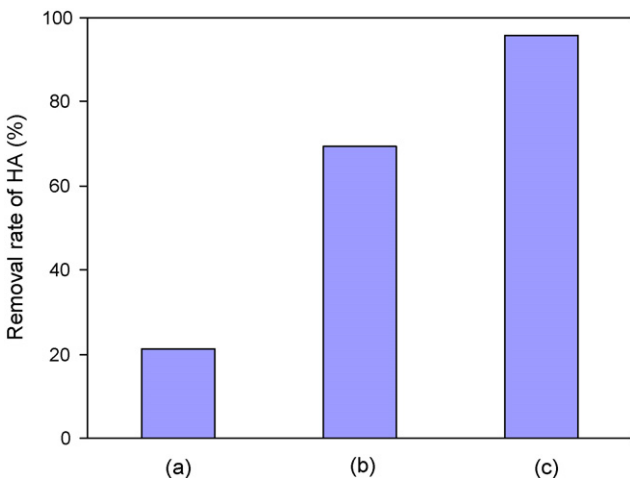


Fig. 10. Removal rates of HA of (a) alumina membrane, (b) TiO₂ nanotube membrane after 2 h of TiO₂ grafting and (c) TiO₂ nanotube membrane after 4 h of TiO₂ grafting. TMP: 0.9 bar.

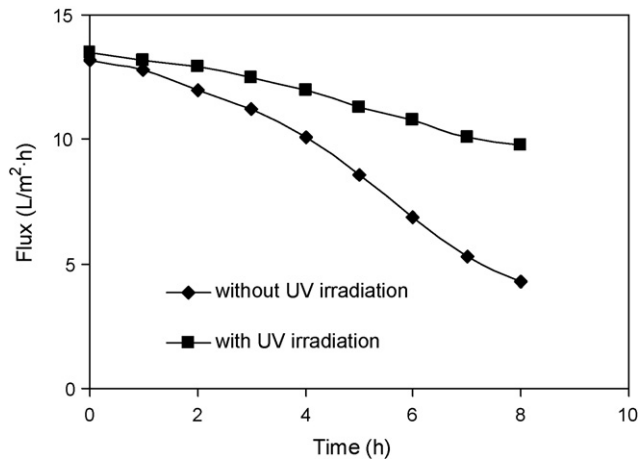


Fig. 11. Changes in membrane flux of the TiO₂ nanotube membrane during filtration of HA. TMP: 0.9 bar.

4. Conclusion

Anatase TiO₂ nanotube membrane has been prepared using TiF₄ solution through liquid-phase grafting on alumina MF membrane. This method is not energy intensive (environmentally friendly) as calcination at high temperatures is not required. TiO₂ nanotubes were grafted into the channels of the alumina membrane template. Membrane pore size can be easily controlled by adjusting the grafting conditions. The fabricated TiO₂ nanotube membrane exhibited good performance on photocatalytic oxidation in removing HA under UV irradiation. Membrane fouling was also alleviated dramatically. The TiO₂ nanotube membrane would have good potential in practical application due to its multifunctional properties, separation, photocatalytic oxidation and anti-fouling.

References

- [1] D.S. Sholl, J.K. Johnson, *Science* 312 (2006) 1003–1004.
- [2] H. Choi, A.C. Sofranko, D.D. Dionysiou, *Adv. Funct. Mater.* 16 (2006) 1067–1074.
- [3] M.R. Hoffmann, S.T. Martin, W. Choi, D.W. Bahnemann, *Chem. Rev.* 95 (1995) 69–96.
- [4] K. Sunada, Y. Kikuchi, K. Hashimoto, A. Fujishima, *Environ. Sci. Technol.* 32 (1998) 726–728.
- [5] J.C. Yu, W. Ho, J. Lin, H. Yip, P.K. Wong, *Environ. Sci. Technol.* 37 (2003) 2296–2301.
- [6] A. Fujishima, T.N. Rao, D.A. Tryk, *J. Photochem. Photobiol. C* 1 (2000) 1–21.
- [7] D.D. Sun, J.H. Tay, K.M. Tan, *Water Res.* 37 (2003) 3452–3462.
- [8] S.Y. Kwak, S.H. Kim, S.S. Kim, *Environ. Sci. Technol.* 35 (2001) 2388–2394.
- [9] M.A. Anderson, M.J. Gieselman, Q. Xu, *J. Membr. Sci.* 39 (1988) 243–258.
- [10] M.D. Moosemiller, C.G. Hill, M.A. Anderson, *Sep. Sci. Technol.* 24 (1989) 641–657.
- [11] H. Choi, E. Stathatos, D.D. Dionysiou, *Desalination* 202 (2007) 199–206.
- [12] G. Trianis, P.J. Evans, D.J. Attard, K.E. Prince, J. Bartlett, S. Tan, R.P. Burford, *J. Mater. Chem.* 16 (2006) 1355–1359.
- [13] W.A. Meulenberg, J. Mertens, M. Bram, H.-P. Buchkremer, D. Stover, *J. Eur. Ceram. Soc.* 26 (2006) 449–454.
- [14] X. Ding, Y. Fan, N. Xu, *J. Membr. Sci.* 270 (2006) 179–186.
- [15] F. Bosc, P. Lacroix-Desmazes, A. Ayral, *J. Colloid Interf. Sci.* 304 (2006) 545–548.
- [16] J. Nishino, C. Information, S. Teekateerawej, Y. Nosaka, *J. Mater. Sci. Lett.* 22 (2003) 1007–1009.
- [17] H.Y. Ha, S.W. Nam, T.H. Lim, I.-H. Oh, S.-A. Hong, *J. Membr. Sci.* 111 (1996) 81–92.
- [18] T. Van Gestel, C. Vandecasteele, A. Buekenhoudt, C. Dotremont, J. Luyten, R. Leyens, B. Van der Bruggen, G. Maes, *J. Membr. Sci.* 207 (2002) 73–89.
- [19] W.P. Yang, S.-L. Huang, *Sep. Sci. Technol.* 38 (2003) 4027–4040.
- [20] Z.-Q. Zeng, X.-Y. Xiao, Z.-L. Gui, L.-T. Li, *Mater. Lett.* 35 (1998) 67–71.
- [21] R. Molinari, L. Palmisano, E. Drioli, M. Schiavello, *J. Membr. Sci.* 206 (2002) 399–415.
- [22] R. Molinari, M. Mungari, E. Drioli, A. Di Paola, V. Loddo, L. Palmisano, M. Schiavello, *Catal. Today* 55 (2000) 71–78.
- [23] I.R. Bellobono, R. Stanescu, C. Costache, C. Canevali, F. Morazzoni, R. Scotti, R. Bianchi, E.S. Mangone, G. de Martini, P.M. Tozzi, *Int. J. Photoenergy* 7 (2005) 109–113.
- [24] I.R. Bellobono, F. Morazzoni, P.M. Tozzi, *Int. J. Photoenergy* 7 (2005) 109–113.

[25] S. Iijima, *Nature* 354 (1991) 56–58.

[26] P.S. Vladimir, N. David, Q. Nicholas, *J. Chem. Phys.* 117 (2002) 8531–8539.

[27] A.I. Skoulios, D.M. Ackerman, J.K. Johnson, D.S. Sholl, *Phys. Rev. Lett.* 89 (2002) 185901–185904.

[28] J.K. Holt, H.G. Park, Y. Wang, M. Stadermann, A.B. Artyukhin, C.P. Grigoropoulos, A. Noy, O. Bakajin, *Science* 312 (2006) 1034–1037.

[29] B.J. Hinds, N. Chopra, T. Rantell, R. Andrews, V. Gavalas, L.G. Bachas, *Science* 303 (2004) 62–65.

[30] M. Majumder, N. Chopra, R. Andrews, B.J. Hinds, *Nature* 438 (2005) 44–44.

[31] M. Adachi, Y. Murata, M. Harada, S. Yoshikawa, *Chem. Lett.* 29 (2000) 942–944.

[32] X. Quan, S. Yang, X. Ruan, H. Zhao, *Environ. Sci. Technol.* 39 (2005) 3770–3775.

[33] J.H. Jung, H. Kobayashi, K.J.C. van Bommel, S. Shinkai, T. Shimizu, *Chem. Mater.* 14 (2002) 1445–1447.

[34] S. Kobayashi, N. Hamasaki, M. Suzuki, M. Kimura, H. Shirai, K. Hanabusa, *J. Am. Chem. Soc.* 124 (2002) 6550–6551.

[35] Z.R. Tian, J.A. Voigt, J. Liu, B. McKenzie, H. Xu, *J. Am. Chem. Soc.* 125 (2003) 12384–12385.

[36] D. Gong, C.A. Grimes, O.K. Varghese, W. Hu, R.S. Singh, Z. Chen, E.C. Dickey, *J. Mater. Res.* 16 (2001) 3331–3334.

[37] G.K. Mor, O.K. Varghese, M. Paulose, N. Mukherjee, C.A. Grimes, *J. Mater. Res.* 18 (2003) 2588–2593.

[38] S.P. Albu, A. Ghicov, J.M. Macak, R. Hahn, P. Schmuki, *Nano Lett.* 7 (2007) 1286–1289.

[39] T. Kasuga, M. Hiramatsu, A. Hoson, T. Sekino, K. Niihara, *Langmuir* 14 (1998) 3160–3163.

[40] Z.-Y. Yuan, B.-L. Su, *Colloid Surf. A* 241 (2004) 173–183.

[41] Y.L. Xiaoming Sun, *Chem. J.* 9 (2003) 2229–2238.

[42] P. Yang, M. Yang, S.L. Zou, J.Y. Xie, W.T. Yang, *J. Am. Chem. Soc.* 129 (2007) 1541–1552.

[43] H.G. Yang, H.C. Zeng, *J. Phys. Chem. B* 107 (2003) 12244–12255.

[44] H. Imai, Y. Takei, K. Shimizu, M. Matsuda, H. Hirashima, *J. Mater. Chem.* 9 (1999) 2971–2972.

[45] H. Imai, M. Matsuta, K. Shimizu, H. Hirashima, N. Negishi, *J. Mater. Chem.* 10 (2000) 2005–2006.